Endogenous Developmental Cycle of the Human Coccidian Cyclospora cayetanensis

Authors: Dubey, J. P., Almeria, S., Mowery, J., and Fortes, J.

Source: Journal of Parasitology, 106(2) : 295-307

Published By: American Society of Parasitologists

URL: https://doi.org/10.1645/20-21

Journal of Parasitology 2020 106(2) 295–307

Published 21 April 2020

DOI: 10.1645/20-21

Contents and archives available through www.bioone.org or www.jstor.org

Journal of Parasitology

journal homepage: www.journalofparasitology.org

ENDOGENOUS DEVELOPMENTAL CYCLE OF THE HUMAN COCCIDIAN *CYCLOSPORA CAYETANENSIS*

J. P. Dubey[1], S. Almeria[2], J. Mowery[3], and J. Fortes[4,5]

[1] United States Department of Agriculture, Agricultural Research Service, Beltsville Agricultural Research Service, Animal Parasitic Disease Laboratory, Building 1001, BARC-East, Beltsville, Maryland 20705-2350.

[2] Department of Health and Human Services, Food and Drug Administration, Center for Food Safety and Nutrition, Office of Applied Research and Safety Assessment, Division of Virulence Assessment, Laurel, Maryland 20708.

[3] United States Department of Agriculture, Agricultural Research Service, Beltsville Agricultural Research Center, Electron and Confocal Microscopy Unit, Building 12, Beltsville, Maryland 20705-2350.

[4] Departamento de Anatomía Patológica, Hospital Universitario Fundación Jiménez Díaz, Universidad Autónoma de Madrid, Spain.

[5] Current Address: Autonomous University of Madrid, Fundacion Jimenez Diaz, Madrid 28040, Spain.

Correspondence should be sent to J. P. Dubey at: *jitender.dubey@usda.gov*

KEY WORDS

Coccidia
Cyclospora cayetanensis
Gamonts
Merozoites
Oocysts
Protozoa
Schizonts

ABSTRACT

Cyclospora cayetanensis is a coccidian parasite of humans of known and growing importance. However, we are surprisingly naïve as to our understanding of how to diagnose it and how it develops inside the human body. Here we provide details of the developmental stages of *C. cayetanensis* in the gallbladder of a 33-yr-old male with human immunodeficiency virus. The gallbladder was removed surgically in 2001 because of severe abdominal pain. For the present study, the archived paraffin block of gallbladder was processed for light microscopy and transmission electron microscopy (TEM). Histological sections were examined after staining with hematoxylin and eosin (HE) or using the periodic acid Schiff (PAS) reaction. Immature and mature asexual stages, gamonts, and oocysts were seen in epithelial cells, both in the superficial epithelium and in glands. The merozoites were present singly, in pairs, and 3 or more in a single parasitophorous vacuole in the host cytoplasm. Up to 6 nuclei were seen in immature schizonts without evidence of merozoite formation. Mature schizonts were 7.6 × 5.1 μm and contained up to 10, 3–4 μm long merozoites. Merozoites were 0.6 to 2.0 μm wide, and their shape varied from pear-shaped to slender. Merozoites were generally PAS-positive; however, some were intensely positive, some had only minute granules, while others were PAS-negative. The microgamonts (male) were 6.6 × 5.2 μm and contained fewer than 20 microgametes around a residual body. The microgametes were up to 2 μm long and were flagellated. Macrogamonts (female) contained distinctive eosinophilic wall-forming bodies that varied in size and were less than 1 μm in HE-stained sections. Macrogamonts were 5.8–6.5 × 5.3–6.5 μm. Oocysts in sections were unsporulated and had a diameter of 5.7–7.5 μm. The TEM examination confirmed the histologic findings. The DNA extracted from paraffin sections was confirmed as *C. cayetanensis* with real-time PCR. The detailed description of the life cycle stages of *C. cayetanensis* reported here in an immunosuppressed patient could facilitate histopathologic diagnosis of this parasite. We have shown that the parasite's development more closely resembles that of *Cystoisospora* than *Eimeria* and that the parasite has multiple nuclei per immature meront indicating schizogony, and we have undermined evidence for a Type II meront.

The coccidian parasite *Cyclospora cayetanensis* can cause serious illness in humans (Ortega et al., 1993, 1997). It has a direct fecal-oral transmission cycle, and the parasite is considered host-specific because no other host besides humans has been identified (reviewed in Almeria et al., 2019; Giangaspero and Gasser, 2019; Li et al., 2020).

The life cycle of *C. cayetanensis* has not been fully described. The oocyst is the only stage definitively identified. After the ingestion of sporulated oocysts in contaminated food, water, or soil by a host, sporozoites are thought to excyst in the gut lumen and invade the enterocytes of the epithelium of small intestine, where the sporozoites round up and subsequently form schizonts, gamonts, and oocysts. Unsporulated oocysts are excreted in feces. The information on the life cycle stages has been derived from piecemeal information by examination of biopsy samples from patients with gastrointestinal disorders. There has been consider-

Table I. Reports of *Cyclospora cayetanensis* stages in intestines of humans in chronological order.

Country of origin	No. of patients	HIV	Biopsy region	Stages in sections	Remarks	Reference
England, holiday travelers in other countries	3	No	Jejunal biopsy in 2, Jejunal juice aspirates in 1	In biopsy in 1, organisms Intracytoplasmic in parasitophorous vacuole in enterocytes, TEM	Holiday travelers from Morocco, Pakistan, and northern India, respectively	Bendall et al. (1993)
Dominican Republic, USA	1	Yes	Duodenum and colon	Immature and mature schizonts, merozoites 6 μm long, TEM		Sun et al. (1996)
Haiti	1	Yes	Duodenum, colon, patient died	Schizonts, merozoites 5–6 μm long		Nhieu et al. (1996)
Peru	17	No	Duodenum and jejunum	Meronts I and II, gamonts, TEM	No. of patients with stages identified unknown, size of asexual and sexual stages unknown, some stages misdiagnosed, see text	Ortega et al. (1997)
USA	2	No	Distal duodenum biopsy	Schizonts, merozoites, TEM Misidentification, see text	No parasites in duodenal aspirate, only 1 merozoite in cross section in 1 patient, Figure 2 mislabeled	Connor et al. (1999)
Argentina	2	Yes	Distal duodenum biopsy	Schizonts with merozoites, light microscopy		Velásquez et al. (2004)
Hong Kong, China	1	Yes	Ileum, colonoscopy	Schizonts, merozoites, in terminal ileum, TEM	No measurements of stages	Tsang et al. (2013)

able confusion concerning the stages found, the terminology used, and the misidentification of stages as evidenced by information summarized in Table I. To our knowledge, details from a complete autopsy have not been previously reported on any case of *C. cayetanensis*.

Unsporulated oocysts have been reported in human sputum, but their sources are unknown (di Gliullo et al., 2000; Hussein et al., 2005). Clinical cholecystitis associated with *C. cayetanensis* infection was reported in 3 patients with human immunodeficiency virus (HIV) infection (Sifuentes-Osornio et al., 1995; de Górgolas et al., 2001). In 2 of these patients, the diagnosis was based on symptoms, ultrasonography, and findings of *C. cayetanensis* oocysts in feces; both cases responded successfully to trimethoprim-sulfamethoxazole treatment (Sifuentes-Osornio et al., 1995). In the third patient, the diagnosis was confirmed histologically (de Górgolas et al., 2001). Here we report details of asexual and sexual development of *C. cayetanensis* in the gallbladder of an HIV-infected patient reported by de Górgolas et al. (2001).

MATERIALS AND METHODS

The subject reported here was a 33-yr-old man from Honduras, described by de Górgolas et al. (2001). Because of severe abdominal pain, the gallbladder was removed surgically. A full-thickness 14 × 3 mm piece was fixed in formalin and embedded in a paraffin block for histopathology. Eighteen years later, the paraffin block and hematoxylin and eosin (HE) -stained section were transported to the senior author's (J. P. D.) laboratory for the present study. To locate the area for transmission electron microscopy (TEM), 3, 5-μm sections were cut and examined microscopically for parasite stages after staining with HE or using the periodic acid Schiff reaction (PAS): sections were then counter-stained with hematoxylin (PASH). From the paraffin block, a 5-mm area was selected for TEM. Several 0.5-μm sections in resin were stained with Toluidine blue. All sections, including the HE-stained slide from Spain, were examined by one of us (J.P.D.) at ×1,000 magnification with an Olympus AX 70 microscope (Olympus Optical Ltd., Tokyo, Japan), stages photographed, and measured using a digital DP73 camera (Olympus Optical Ltd.). The number of merozoites within a schizont was determined by counting the nuclei.

For TEM, paraffin-embedded tissue was de-paraffinized and processed for thin sectioning. Tissue was fixed in 1% buffered osmium tetroxide for 2 hr at room temperature. The tissue was then rinsed 6 times in the same buffer, dehydrated in a graded ethanol series followed by 2 exchanges of propylene oxide, infiltrated in a graded series of LX-112 resin/propylene oxide, and polymerized in LX-112 resin at 65 C for 24 hr. Sixty to 90 nm silver-gold sections were cut on a Reichert/AO Ultracut ultramicrotome (Leica Microsystems, Buffalo Grove, Illinois) with a Diatome diamond knife and mounted onto 200 mesh formvar-coated copper grids. Grids were stained with 4% uranyl acetate and 3% lead citrate and imaged at 80 kV with a Hitachi HT-7700 (Hitachi High Technologies America, Schaumburg, Illinois) transmission electron microscope.

Molecular confirmation of *C. cayetanensis*

DNA from 3, 5-μm paraffin sections containing parasites was extracted following the commercial QIAmp-DNA-FFPE-tissue kit (Qiagen, Valencia, California). A real-time PCR for *C. cayetanensis 18S rRNA* gene (modified from Verweij et al., 2003) and an internal amplification control (IAC) was performed on an Applied

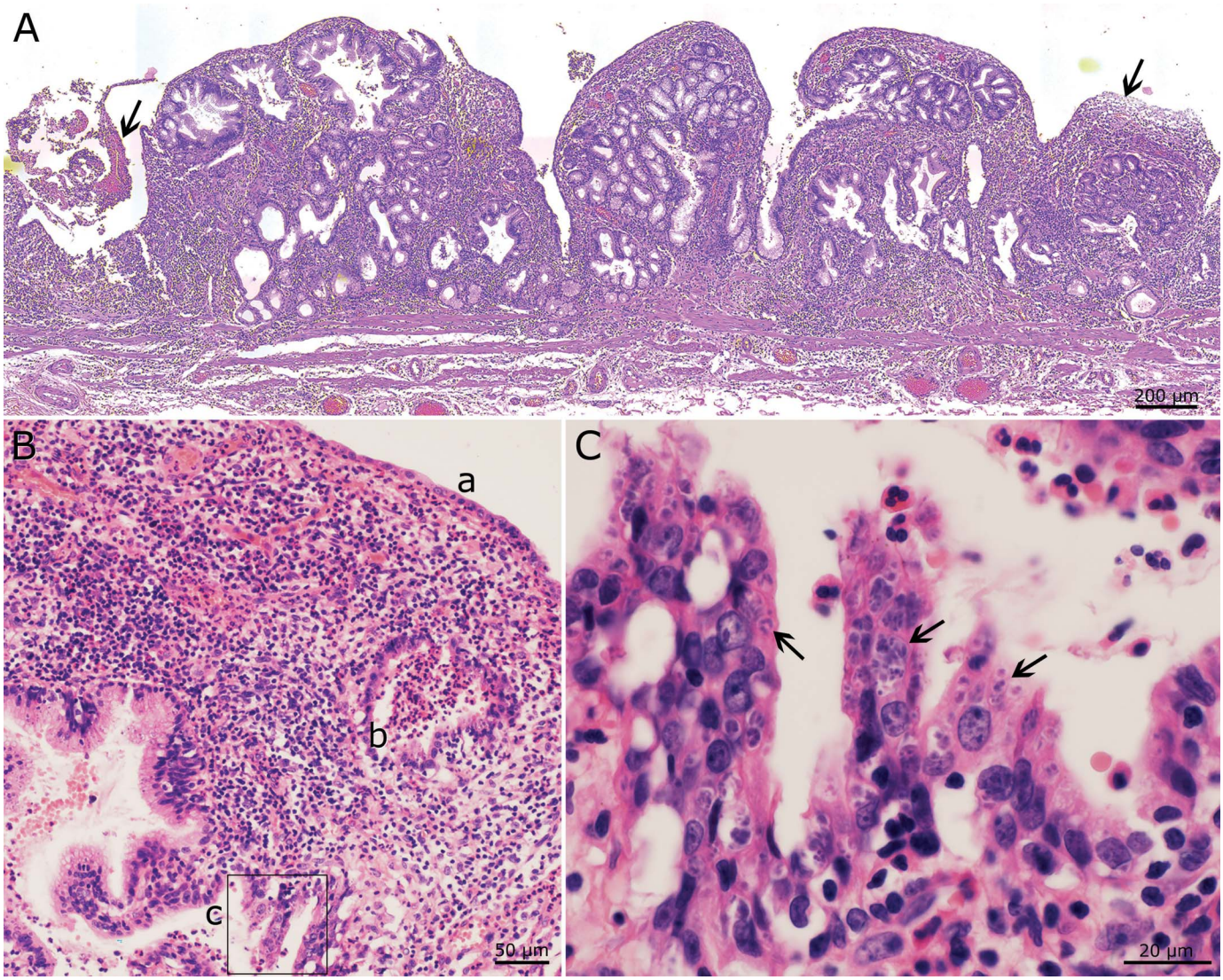

Figure 1. Histological section (5 µm) of gallbladder of the HIV patient infected with *Cyclospora cayetanensis*. Hematoxylin and eosin stain. (**A**) Focal ulceration (arrows) and severe transmural inflammation. (**B**) Intact surface epithelium (a), exudation and sloughing in the lumen of a gland (b), and infected epithelium (c). (**C**) Higher magnification of the marked area from Fig. 1B-c. Note severe parasitism of epithelium (arrows). Color version available online.

Biosystems 7500 Fast Real-time PCR System (ThermoFisher Scientific, Waltham, Massachusetts) using the primers and probes and conditions indicated by Murphy et al. (2017). Briefly, the experimental real-time PCR run consisted of the study sample, a non-template control (NTC), and positive controls containing 10-fold serial dilutions from 10^3 to 10 copies of a commercially prepared synthetic gBlocks gene fragment (HMgBlock135, Integrated DNA Technologies, Coralville, California) for amplification of the *C. cayetanensis 18S rRNA* gene (Murphy et al., 2017). Reactions were individually performed using 2.0 µl of template and controls in a final reaction volume of 20 µl. The amplification protocol consisted of an initial step of 95 C for 5 min followed by 45 cycles of 95 C for 30 sec and 67 C for 30 sec. Data were collected during the 67 C step. The analysis was performed using the Applied Biosystems 7500 Software v.2.3 (https://www.thermofisher.com/us/en/home/technical-resources/software-downloads/applied-biosystems-7500-real-time-pcr-system.html) provided by the real-time manufacturer, with a baseline setting from 6 to 15 cycles and a threshold of 0.2 for both target reactions. Samples were analyzed in triplicate reactions. Samples were considered positive if one or more replicates produced a *C. cayetanensis* target reaction with a C_T value less than or equal to 38.0. Reactions would have been considered inconclusive if the IAC reaction failed or produced an average C_T value of more than 3 cycles higher when compared to the NTC; however, this was not observed in the present study.

RESULTS

The gallbladder was thickened and focally ulcerated, and parasite stages were present in the epithelium, sub-epithelial glands, and lumen of glands and gallbladder (Figs. 1A-C; 2A, B). Parasites multiplied only in epithelial cells. Parasite stages were located above or below the host cell nucleus, and the host cell nucleus was indented but not hypertrophied (Fig. 2F). All stages

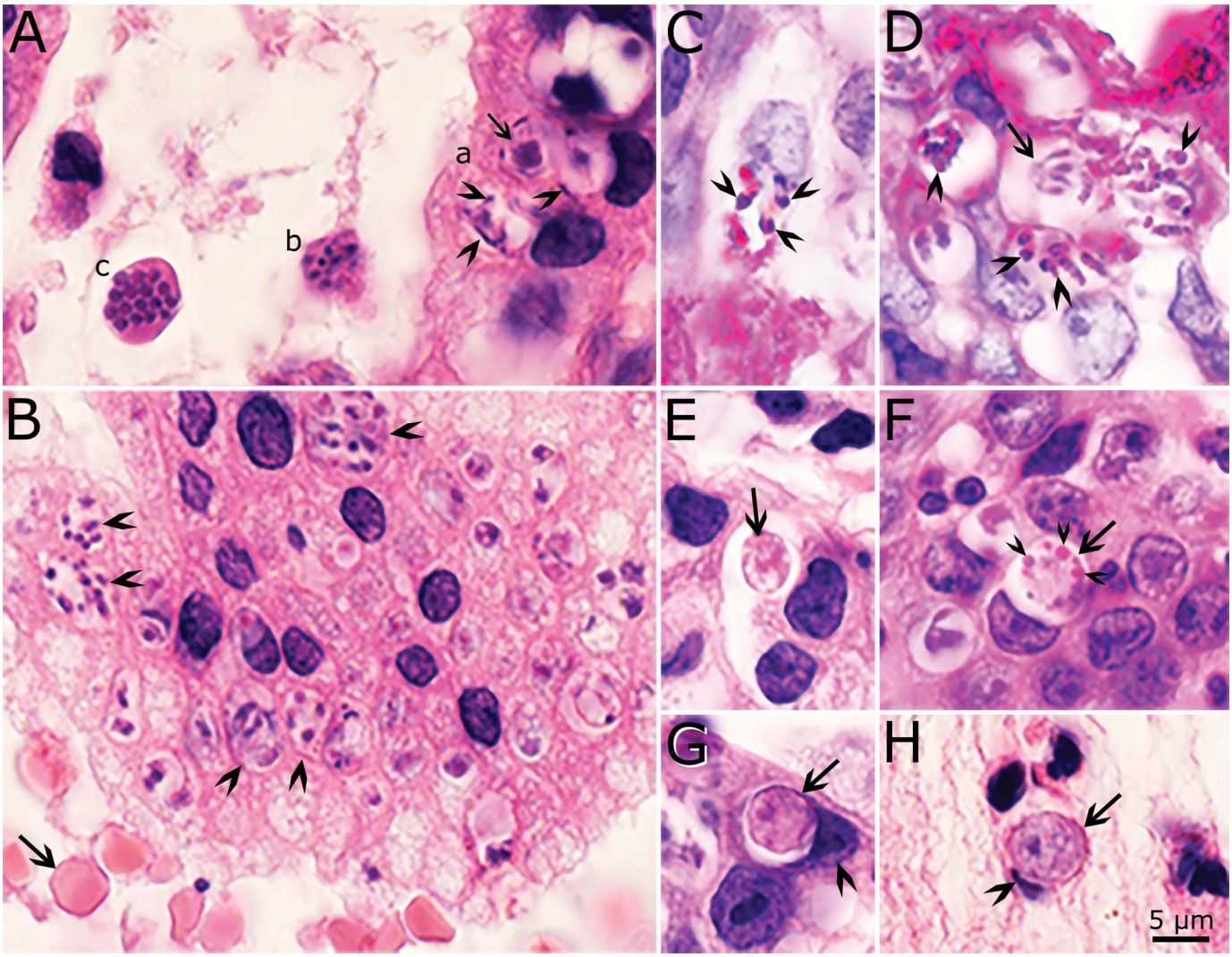

Figure 2. Higher magnification of the gallbladder in Figure 1 showing stages of *Cyclospora cayetanensis*. (**A, B, E, F, G, H**) Hematoxylin and eosin stain. (**C, D**) Periodic acid Schiff (PAS) reaction, counter-stained with hematoxylin. Bar applies to all figures. (**A**) The glandular epithelium is on the right and lumen on the left. (a) Three microgamonts in epithelial cells. Note peripherally located microgametes (arrowheads) around a large residual body (arrow). (b, c) Schizonts free in the lumen of a gland. Note cross section (c) of merozoites in a schizont. (**B**) Desquamated epithelium in lumen of a gland. Note numerous schizonts (arrowheads) and red blood cells (arrow) for size comparison. (**C**) A schizont with PAS-positive (arrowheads) merozoites. (**D**) Several schizonts with variable PAS-positive granules (arrowheads). Arrow points to a PAS-negative schizont that has merozoites attached to a residual body (arrow). (**E**) An early macrogamont (arrow). (**F**) A late macrogamont (arrow) with eosinophilic wall-forming bodies (arrowheads). The host cell nucleus is indented. (**G**) An intracellular oocyst (arrow) in the epithelium. Note indented host cell nucleus (arrowhead). (**H**) An oocyst (arrow) free in lumen of gallbladder. Arrowhead points to indented host cell nucleus. Color version available online.

were in the host cytoplasm within a parasitophorous vacuole (pv). Schizonts, gamonts, and oocysts could be identified in HE or PASH-stained histological sections (Fig. 2A–H). Merozoites were generally PAS-positive; however, some were intensely positive, some had only minute granules, while others were PAS-negative (Fig. 2C, D).

More parasite details became clear in 0.5-µm-thick sections stained with Toluidine blue (Figs. 3, 4). To facilitate diagnosis, different shapes and sizes of schizonts and merozoites are illustrated in Figures 3 and 4. Most of the stages seen were asexual. The earliest stage was a uninucleate round or oval stage (Fig. 3B), but it was unclear if this stage was a precursor of schizonts or gamonts. Immature schizonts contained 2–6 nuclei without evidence for merozoite formation (Fig. 3A–D, J, K). Schizonts were circular to elongated in shape (Figs. 3A, I, J; 4D, E). Some schizonts contained a residual body (Fig. 4A–D) whereas most did not. The number of generations of schizogony was not determined because of profuse multiplication and the variability of structures of schizonts and merozoites.

Most schizonts were mature and contained 2 or more merozoites. It was difficult to count merozoites unless the nuclei were within the 1 plane of focus; a maximum of 10 merozoites could be definitively identified. Most merozoites in schizonts were arranged loosely with spaces between merozoites (Figs. 3A, H; 4D). Mature schizonts were 7.6 × 5.1 µm (3.2–13.9; n = 67). Merozoites were 0.6 to 2.0 µm wide, and their shape varied from pear-shaped to slender (Figs. 3E–G, I; 4E–H). Only a few multinucleated stages (immature) schizonts were seen (Fig. 3A,

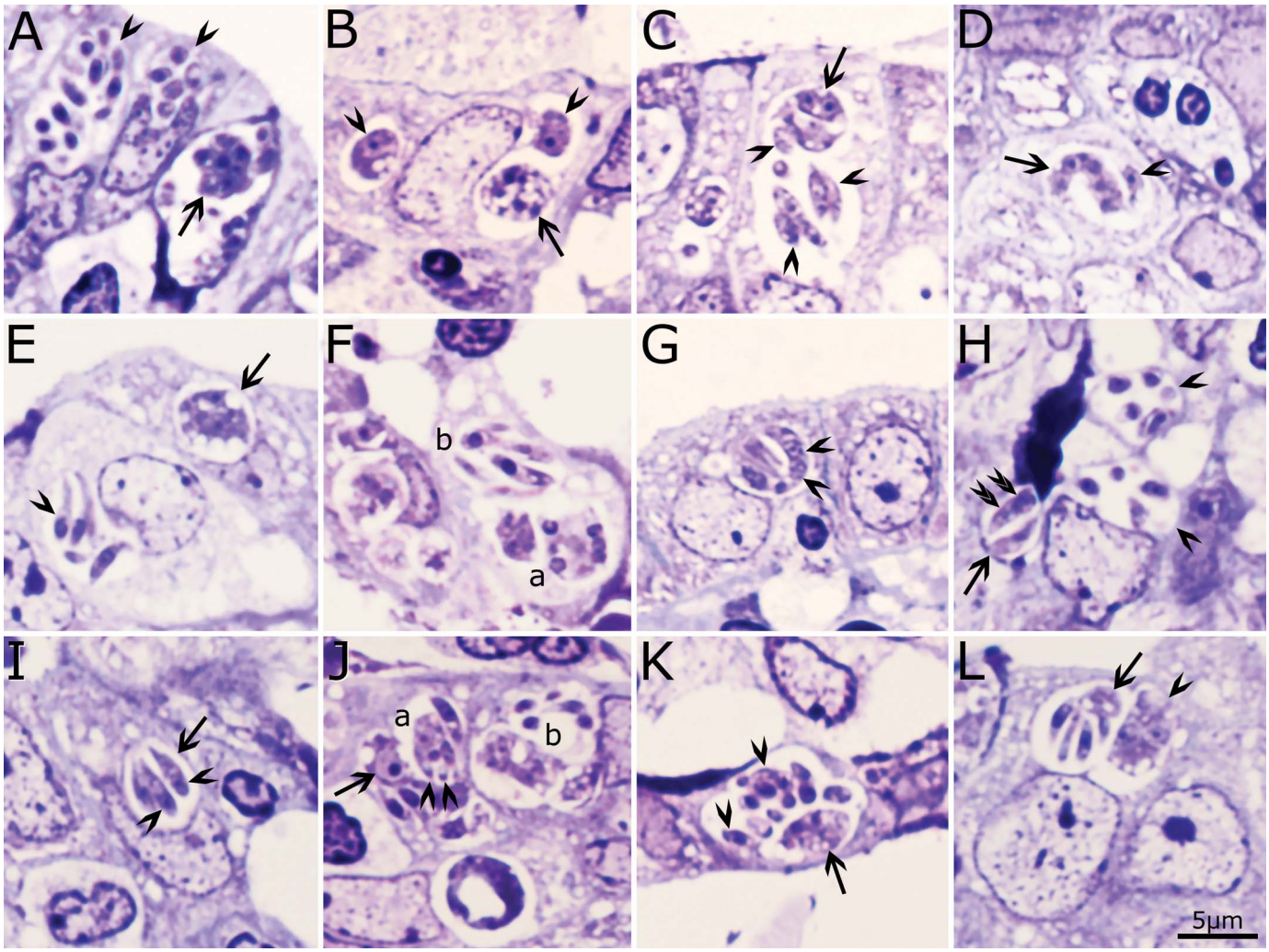

Figure 3. Asexual stages of *Cyclospora cayetanensis* in 0.5-μm sections of gallbladder. Toluidine blue stain. Bar applies to all figures. (**A**) Three schizonts. Arrowheads point to mature schizonts in surface epithelium. Arrow points to a group of parasites with an immature schizont with at least 6 nuclei; several merozoites are also present in the same vacuole. (**B**) Two uninucleate organisms with a large nucleolus (arrowheads) and an immature schizont with 5 nuclei (arrow). (**C**) A parasitophorous vacuole (pv) containing a group of organisms. Note a binucleate organism (arrow) and several merozoites that appear to have more than 1 nucleus (arrowheads). (**D**) An irregular-shaped schizont with 5 nuclei (arrow) and 1 separate uninucleate structure (arrowhead). (**E**) A schozont with 5 nuclei and merozoite ends at the periphery (arrow). Also, note a mature schizont with 4 merozoites (arrowhead). (**F**) Parasites in different stages of development. (a) Multinucleate structure and (b) schizont with merozoites, one of which has terminal nucleus. (**G**) A schizont-like structure with 1 crescent-shaped organism with at least 2 nuclei (arrowheads). (**H**) Two mature schizonts (arrowheads) and 2 parasites in another group (arrow) containing 2 merozoite-like structures, one of which has 2 nuclei (double arrowheads). The dark blue staining structure is artifact of staining. (**I**) Schizont (arrow) with 3 merozoites. Note terminal nuclei (arrowheads). (**J**) Two groups of schizonts. (a) A multinucleated schizont with merozoites protruding (arrowheads). (b) A vacuole with free merozoites and an undivided mass. Arrow points to a macrogamete-like structure. (**K**) A parasitophorous vacuole (pv) that has a multinucleated immature schizont (arrow) and several mature merozoites (arrowheads). (**L**) A schizont with merozoites attached to a residual body (arrow). Note central location of nucleus in a merozoite. Also, note a multinucleated structure (arrowhead) apparently in the same pv. Color version available online.

K). The staining of merozoites was variable, some were faintly stained (Fig. 3C, I), whereas others were stained intensely (Fig. 4A, G). The position of nucleus varied from being terminal to central (Figs. 3A, L; 4F, G). The nucleus in some merozoites was vesicular (Fig. 3C, I). Merozoites had pointed or blunt ends (Figs. 3E, F, I, L; 4A, H).

Compared to schizonts, only a few gamonts were identified. The microgamonts (male) were 6.6 × 5.2 (4.2–9.0 × 4.0–6.6; n = 18) μm and contained fewer than 20 microgametes. The nuclei in microgamonts had condensed chromatin, and they were peripherally arranged (Fig. 4I, J). An eosinophilic residual body, up to 4 μm wide, was seen in some microgamonts (Fig. 2 A). The microgametes were up to 2 μm long.

In HE-stained sections, macrogamonts (female) contained distinctive eosinophilic wall-forming bodies (WFBs) that varied in size and were less than 1μm. The macrogamonts with WFBs were 6.4 × 5.6 (5.8–7.3 × 5.2–6.4; n = 5) μm (Fig. 2F). Oocysts in sections were 6.6 × 5.9 (6.0–7.5 × 5.6–6.4, n = 5) μm; they had a crumpled wall and were identified only in HE-stained sections (Fig. 2H).

With TEM, the preservation was sub-optimal but still allowed certain aspects to be examined but not the ultrastructural details.

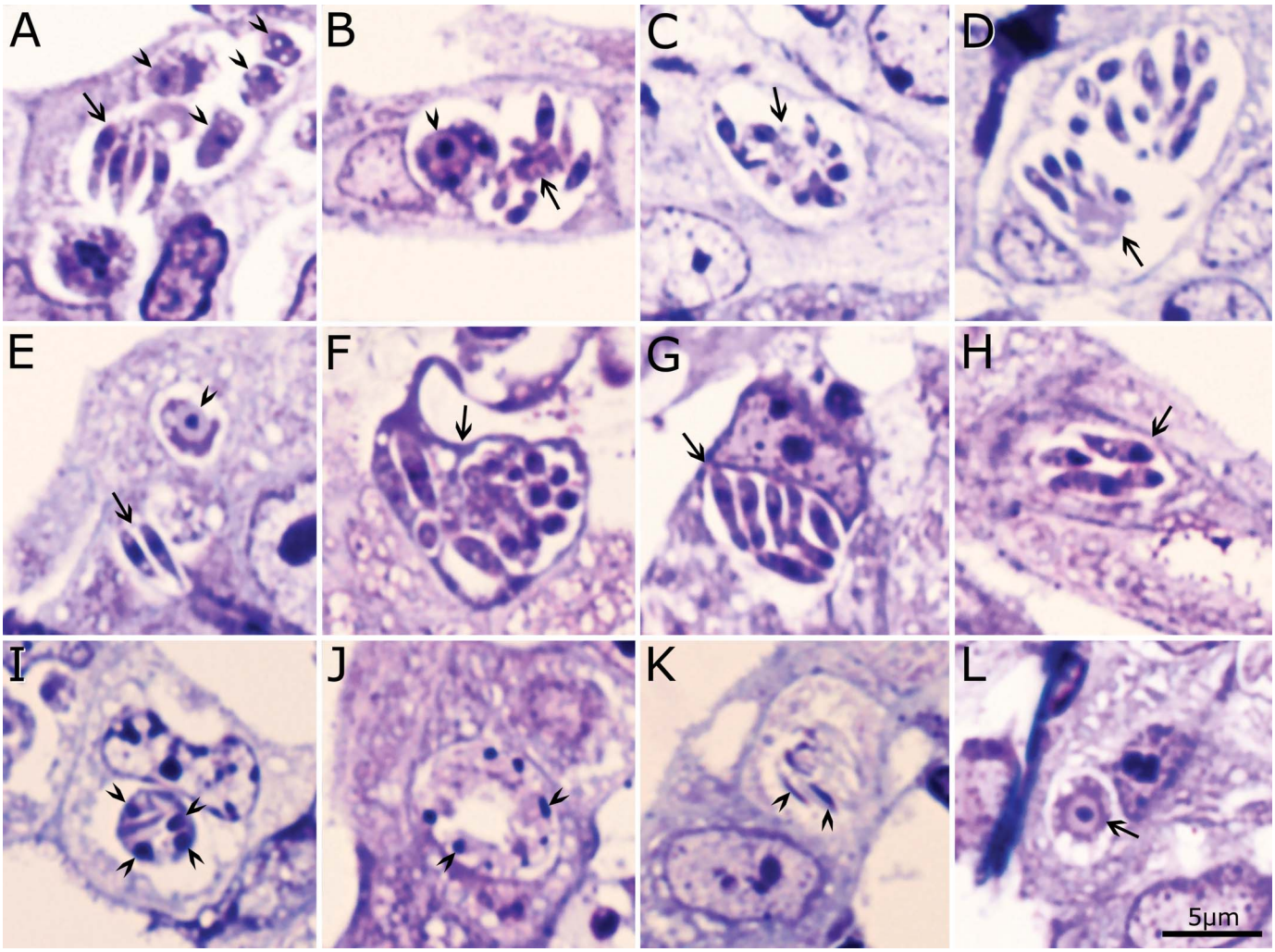

Figure 4. Asexual and sexual stages of *Cyclospora cayetanensis* in 0.5-µm sections of gallbladder. Toluidine blue stain. Bar applies to all figures. (**A**) Several parasite groups in a parasitophorous vacuole (pv). Arrow points to longitudinally cut merozoites attached to a residual body. Arrowheads point to macrogamont-like structures (**B**) A pv containing merozoites attached to a residual body (arrow) and 2 macrogamont-like structures (arrowhead). (**C**) Nearly mature schizont (arrow) with merozoites in different plane of section. (**D**) Two groups of merozoites apparently in 1 pv, in 1 group merozoites are attached to a residual body (arrow). This is the largest schizont found. (**E**) Two merozoites in a pv and a macrogamont (arrowhead). (**F**) Longitudinal and cross sections of merozoites in a schizont (arrow). (**G**) A schizont (arrow) with 7 merozoites that are intensely stained. (**H**) A schizont (arrow) with banana-shaped merozoites. (**I**) Microgamont with 4 nuclei (arrowheads). (**J**) Microgamont with peripherally arranged nuclei (arrowheads). (**K**) Microgametes (arrowheads). (**L**) A macrogamont (arrow) with a large central nucleus and a large nucleolus. Color version available online.

Also with TEM, all stages were in pv of epithelial cells (Figs. 5–12). Most parasites studied were schizonts. Immature schizonts contained 2–5 nuclei without evidence of merozoite formation (Fig. 5A–D). The nuclei of immature schizonts had dispersed chromatin and prominent nucleolus (Fig. 5B). Figure 6 shows 3 schizonts in different stages of development. Figure 7 shows an immature schizont with merozoites arising at the periphery of a prominent residual body. Figure 8 shows a longitudinally cut merozoite attached to a residual body. The merozoites varied in shape, structure, and size (Figs. 9–11). One group of merozoites contained numerous amylopectin granules (Fig. 10). Numerous dense granules-like structures were found in a schizont (Fig. 11).

Only a few gamonts were identified by TEM. Figure 12A shows an immature microgamont with 7 peripherally arranged nuclei; the nuclear chromatin in the nuclei was condensed at the periphery of the nuclei. Free flagella were present at the periphery of a mature microgamont (Fig. 12B). The flagella were 200 nm in diameter (Fig. 12B).

The macrogamonts had electron-dense wall-forming bodies 1 (WFB1) and electron-lucent WFB2; these WFBs were 40–144 nm in diameter (Fig. 12C, D).

The proposed life cycle of *C. cayetanensis* is diagrammatically presented in Figure 13.

Molecular detection by real-time PCR from DNA extracted from tissue sections confirmed the presence of *C. cayetanensis* in the tissue, with an average C_T value of 34.7 ± 0.1 for *C. cayetanensis 18S rRNA* gene in the sample.

Specimens deposited

Toluidine blue-stained and hematoxylin and eosin-stained histological sections of gallbladder of the patient were deposited in the United States National Parasite Collection in the Division

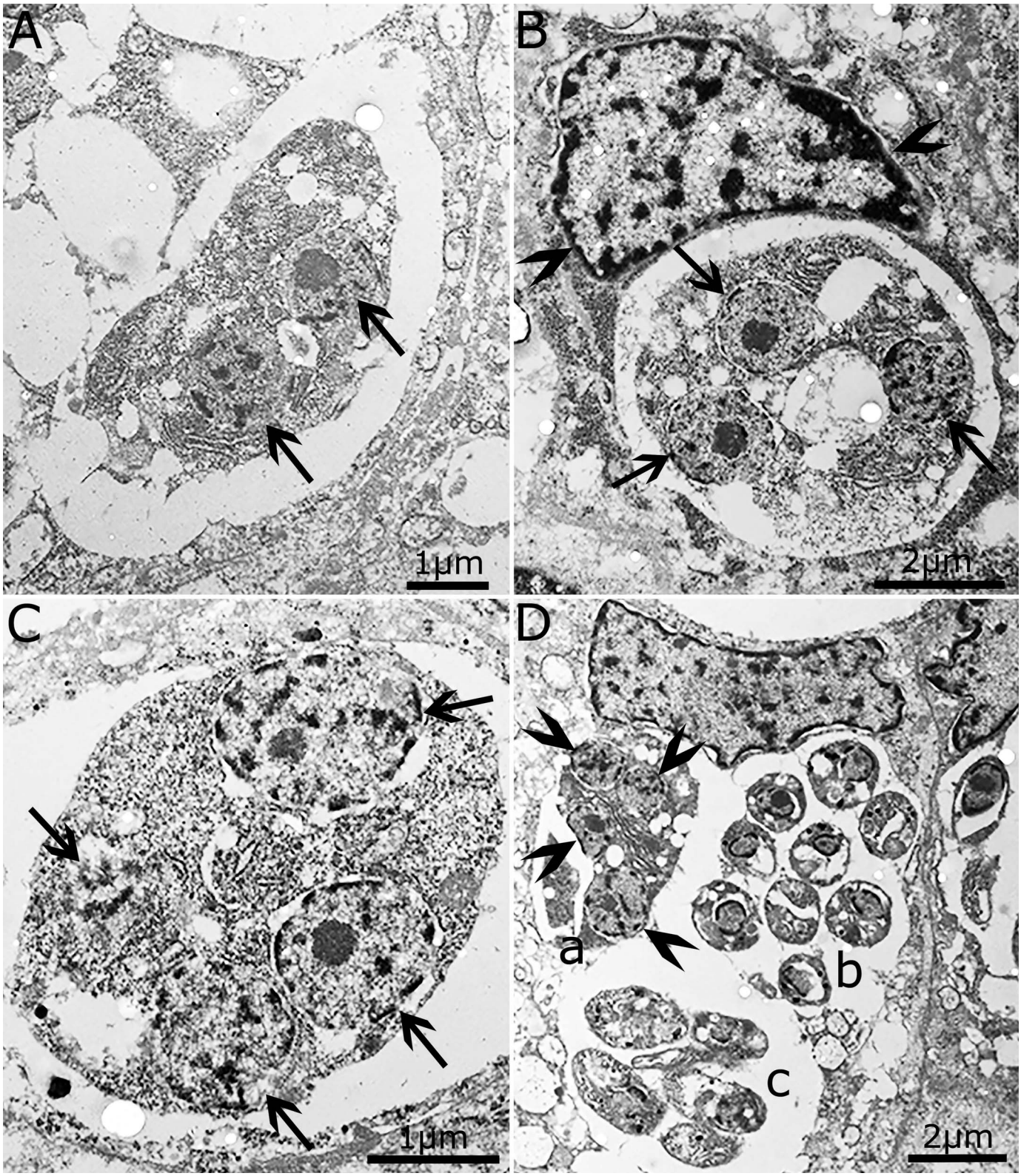

Figure 5. Transmission electron micrographs of schizonts of *Cyclospora cayaetanensis*. (**A**) Schizont with 2 nuclei (arrows). (**B**) Immature schizont with 3 nuclei (arrows). Note the nuclei have a prominent nucleolus and the chromatin is dispersed. Also, note indented host cell nucleus (arrowheads). (**C**) Immature schizont with 4 nuclei (arrows). (**D**) Three groups of schizonts apparently within 1 epithelial cell. (a) Immature schizont with 4 nuclei (arrowheads). (b) Cross sections of merozoites in a mature schizont. (c) Five merozoites in another group.

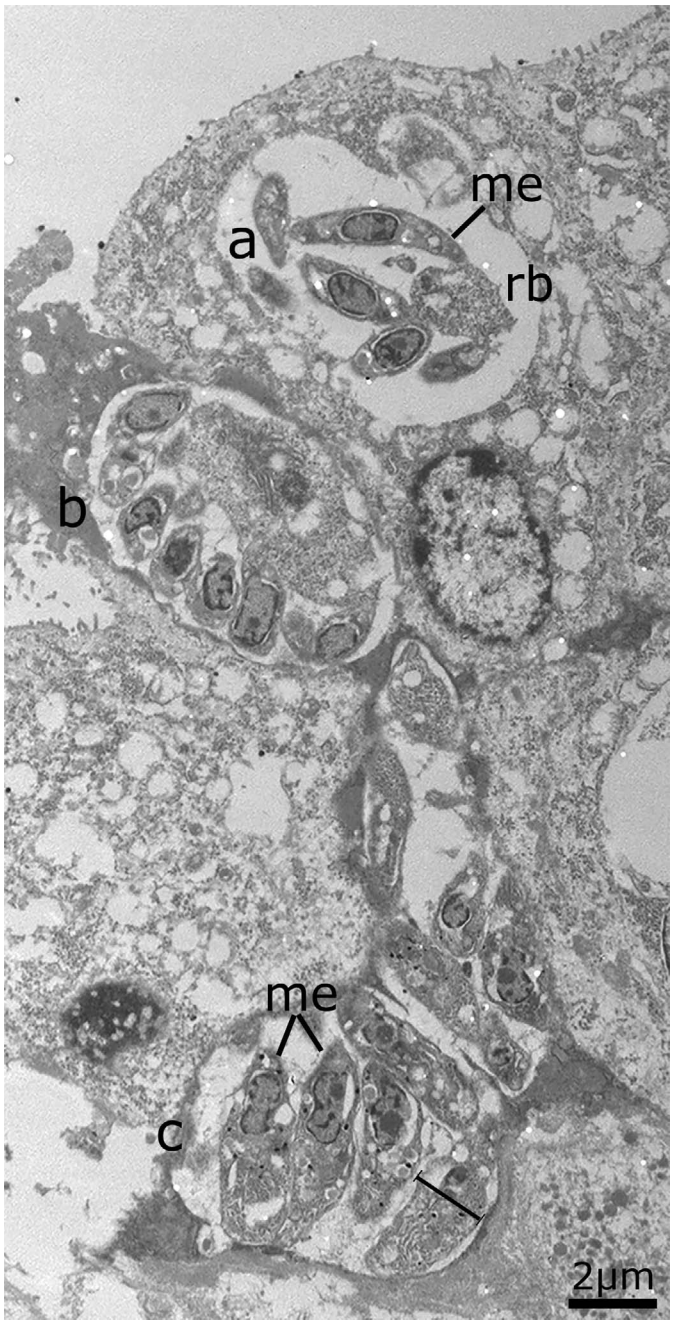

Figure 6. Transmission electron micrograph of schizonts of *Cyclospora cayetanensis*. (a) Schizont with merozoites (me) around a residual body (rb). (b) Immature schizont. (c) Mature schizont. The merozoites (me) in this schizont are about twice wider than the slender merozoite in shizont a.

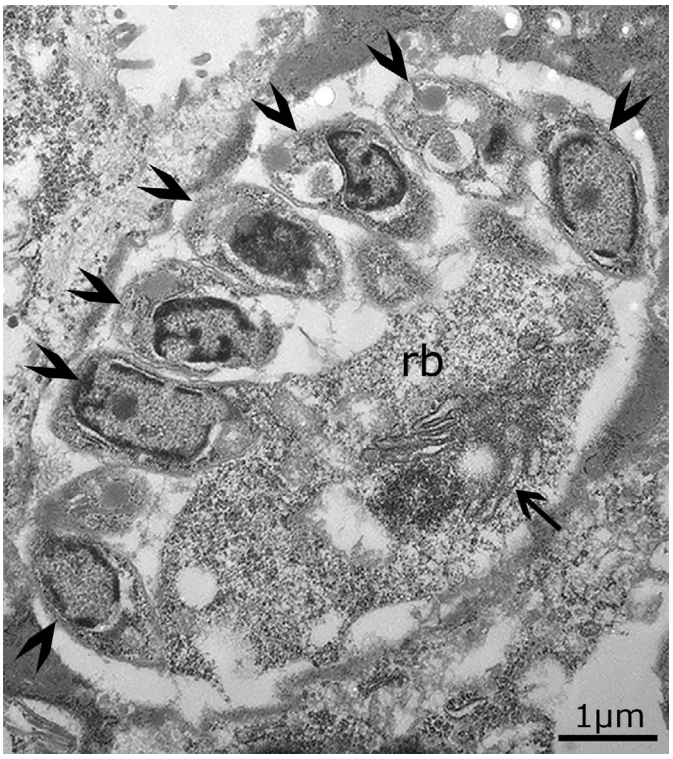

Figure 7. Transmission electron micrograph of an immature schizont (arrow) of *Cyclospora cayetanensis*. Higher magnification of the schizont in Figure 6b. Note merozoites (arrowheads) arising at the periphery of a prominent residual body (rb, arrow).

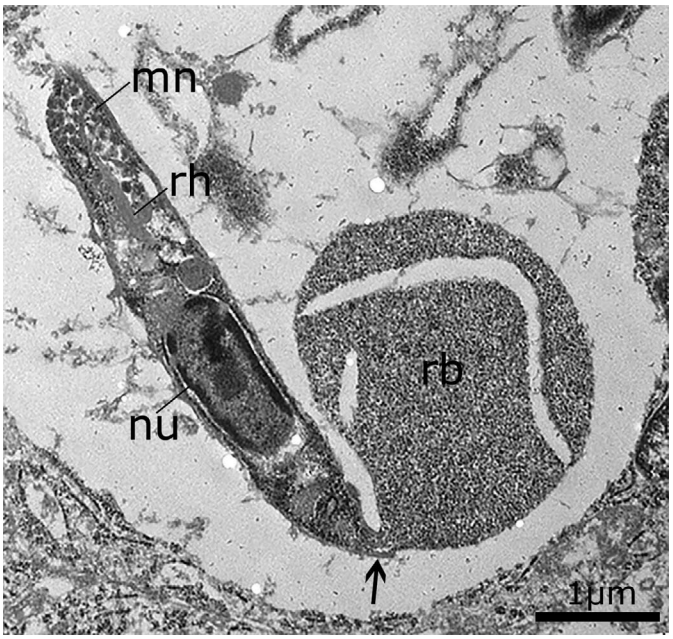

Figure 8. Transmission electron micrograph of an immature schizont of *Cyclospora cayetanensis*. A slender merozoite attached (arrow) to a residual body (rb). Note micronermes (mn), a rhoptry (rh), and a prominent nucleus (nu).

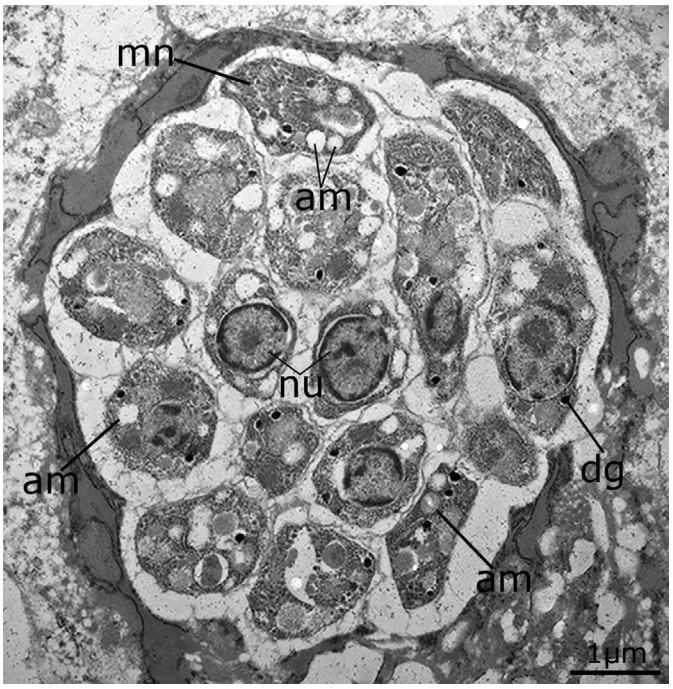

Figure 9. Transmission electron micrograph of a mature schizont of *Cyclospora cayetanensis*. Note micronemes (mn), nucleus (nu), amylopectin granules (am), and dense granules (dg).

Figure 11. Transmission electron micrograph of a mature schizont of *Cyclospora cayetanensis*. Note numerous dense granules-like structures (dg) located anterior and posterior to nucleus (nu). Also, note micronemes (mn) at the apical ends of merozoites.

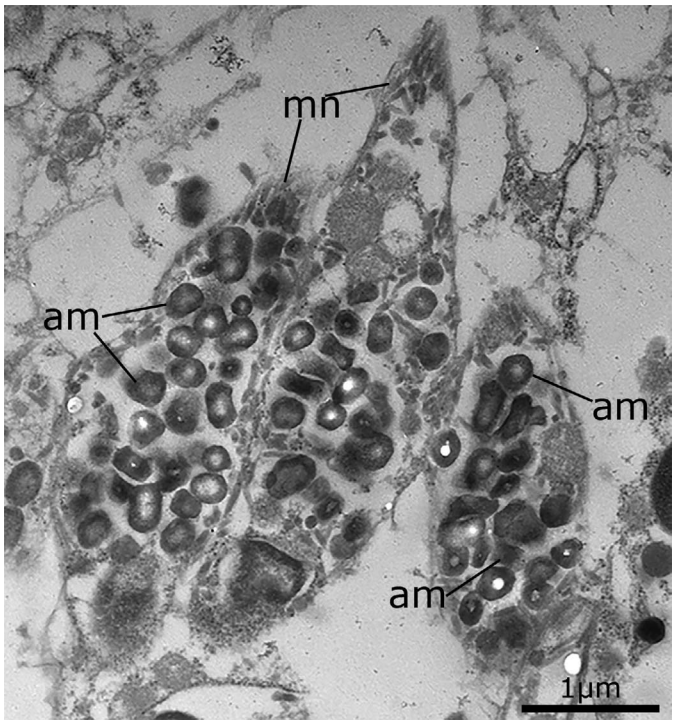

Figure 10. Transmission electron micrograph of 3 merozoites of *Cyclospora cayetanensis*. Note numerous amylopectin granules (am) and few micronemes (mn).

of Invertebrate Zoology and National Museum of Natural History, Smithsonian Institution, Museum Support Center, MRC 534, 4210 Silver Hill Road, Suitland, Maryland 20746, under numbers USNM-1614395 and 1614396.

DISCUSSION

There is considerable confusion concerning the terminology used to describe endogenous stages of coccidia, including *C. cayetanensis* (see Table I). The term *trophozoite* used by some authors is unclear. Before the discovery of the coccidian phase (oocyst) of *Toxoplasma gondii* in 1970, the term was used to denote the initial intracellular stage of coccidia (*Eimeria*). In an eimerian life cycle, after entry of sporozoite or merozoite in the host cell, sporozoites/merozoites round up and lose many of their organelles. This stage has been called the trophozoite. The term *uninucleate zoite* is preferred now because the trophozoites of *Eimeria* are nonmotile and contain a single nucleus; using this term avoids confusion with the motile trophozoites of other protozoa, which may contain 2 nuclei; stages called trophozoites in *T. gondii* differ structurally from those termed trophozoites in *Eimeria* (Dubey et al., 2020). The terms *endodyogeny, schizogony,* and *merogony* have been used to describe asexual division in coccidia. Some coccidian species can divide into 2 merozoites, probably by endodyogeny. However, most species of intestinal coccidia divide by schizogony—a process in which the nucleus divides into 4 or more nuclei before merozoites are formed (Dubey et al., 2020). We use the term *schizont* here irrespective of the mode of division. Some authors use the terms *merogony* or *meronts,* which is not specific to endodyogeny or schizogony.

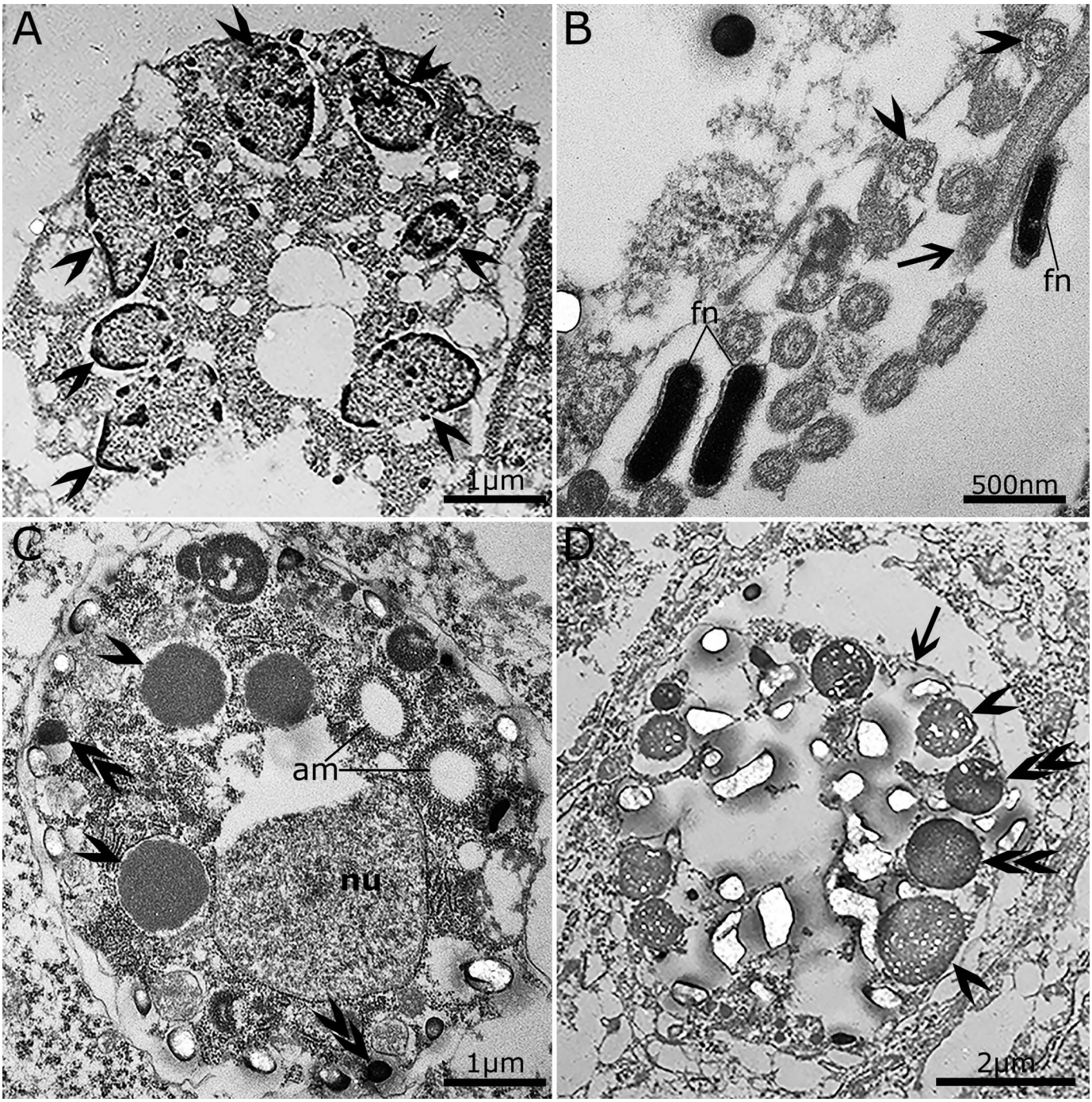

Figure 12. Transmission electron micrographs of gamonts of *Cyclospora cayetanensis*. (**A**) A microgamont-like structure with 7 peripherally located nuclei. Note that the chromatin (arrowheads) is arranged at the periphery of nuclei. (**B**) Flagella at the periphery of the microgamont. Arrow points to longitudinal section and arrowheads point to cross sections of flagella. Note the elongated flagellar nucleus (fn). (**C**) Macrogamont with a nucleus (nu) and wall-forming bodies 1 (WFB1) (arrowheads) and electron dense WFB2 (arrows). Also, note amylopectin granules (am). (**D**) A macrogamont (arrow) with WFB1 (double arrowheads) and WFB2 (arrowheads).

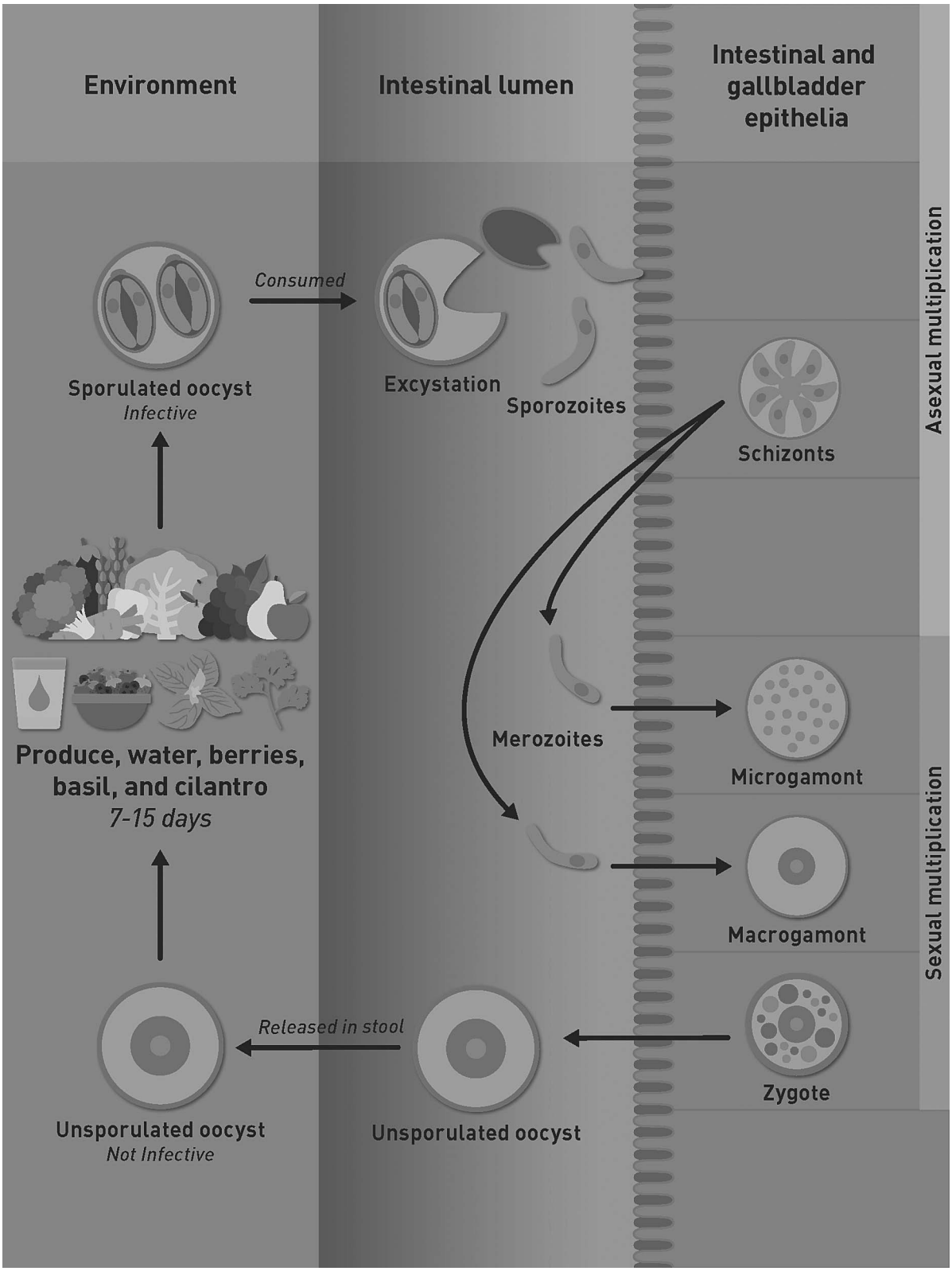

Figure 13. Proposed life cycle of *Cyclospora cayetanensis*. Modified from Almeria et al. (2019).

Here we documented schizogony in *C. cayetanensis* for the first time. The evidence for this was observing 5 or more nuclei in immature schizonts prior to merozoite formation. Additionally, a distinct residual body was seen in some schizonts, suggesting a different generation. In the present study, some host cells had 2 merozoites; it was not determined if they had divided by endodyogeny or were a different generation, or whether 2 merozoites had entered 1 host cell at different periods. The mode of division of schizonts in *C. cayetanensis* appears to be different from that in *Eimeria* species. In *Eimeria* species, merozoites released from schizonts enter new host cells to form schizonts or gamonts. However, in the patient reported here, immature *C. cayetanensis* schizonts were present along with mature merozoites in the same host cell. This type of division resembles that observed in species of *Cystoisospora* infecting dogs, cats, and humans (Dubey et al., 2020). These observations in this case of heavy *C. cayetanensis* infection warrant confirmation. In cases where it could be ruled out that multiple merozoites could have entered the same host cell, the typical developmental picture could be better defined.

Ortega et al. (1997) first proposed the concept of 2 types of meronts in *C. cayetanensis*. Type I meronts had small (3–4 × 0.5 μm), 8–12 merozoites, and Type II meronts had 4 long (12–15 × 0.7–0.8 μm) merozoites. The dimensions of meronts were not given. It was also not clear how often Type II meronts were seen (Ortega et al., 1997). The illustration of Type II merozoites in the paper by Ortega et al. (1997) has no scale bar or magnification, and, thus, it is difficult to verify the size; we are aware of no archived specimens available for verification. Type II meronts were not detected in the present case that had profuse growth of schizonts and sexual stages. Type II meronts (with long merozoites) also were not reported from any of 5 other papers (summarized in Table I); the merozoites reported in these studies were 3–6 μm. Judging by the size of merozoites illustrated in Fig. 5B of Ortega et al. (1997), the meront is likely Type I. Upon reflection and in the light of our observations, we conclude that the stage labeled as a trophozoite in Figure 5A of Ortega et al. (1997) ought instead to be understood as the conoidal end of a merozoite with numerous micronemes and a rhoptry; trophozoites, by contrast, have only a few organelles (Dubey et al., 2020).

The gamonts of *C. cayetanensis* found in the present study were very small; their dimensions were not provided previously including the seminal report of Ortega et al. (1997). Compared with schizonts, only a few gamonts were found. The macrogamonts could be recognized by the presence of WFBs. We provide here the first illustration of macrogamonts in histologic sections stained by HE; these had characteristic eosinophilic WFBs. Using TEM, the 2 types of WFBs could be distinguished by their density: WFB1 were electron-dense, whereas WFB2 were electron-lucent—this was illustrated in an excellent image (Fig. 5C) by Ortega et al. (1997); however, amylopectin granules were mislabeled as WFBs. We also illustrate here for the first time *C. cayetanensis* unsporulated oocysts in HE-stained sections.

The microgamonts of *C. cayetanensis* are also small and contain few microgametes (<20). Early stages of microgamonts are difficult to distinguish from immature schizonts. However, the nuclei in microgamonts are arranged peripherally and the chromatin is also at the periphery of the nuclei, whereas in schizonts the nuclei are generally arranged centrally and the chromatin is dispersed. Here we demonstrate for the first time that the microgametes of *C. cayetanensis* have flagella.

The unsporulated oocysts of *C. cayetanensis* in fresh feces are 8–10 μm in diameter (Almeria et al., 2019); their dimensions in histological sections have not been reported before. In the immunosuppressed patient reported here, *C. cayetanensis*–like oocysts were found in bile drainage; the oocysts in Ziehl-Neelsen–stained smears were pink and 10 μm in diameter (de Górgolas et al., 2001). Here, in histological sections of the gall bladder, unsporulated oocysts were 5.7–7.5 μm in diameter; the smaller size was probably due to shrinkage during fixation in formalin and paraffin embedding. As stated in the introduction, the life cycle of *C. cayetanensis* is not fully understood. Sporulation of oocysts occurs outside the host. After ingestion, oocysts excyst in the gut lumen and the parasite multiplies in enterocytes. Judging from the biopsy reports listed in Table I, *C. cayetanensis* parasitizes enterocytes throughout the small intestine. How the parasite reaches the biliary tract and gallbladder is unknown. It is likely that some sporozoites/merozoites from intestinal lumen are spilled in the bile duct and invade the biliary tract. Whether this is part of the life cycle or aberrant parasitism that occurs in immunocompetent patients is unknown.

The parasitic stages of *C. cayetanensis* are one of the smallest in size among coccidian parasites. *Cystoisospora belli* is the other coccidian known to parasitize intestines, bile ducts, and gallbladder of humans (Dubey and Almeria, 2019). However, schizonts and gamonts of *Cystoisospora belli* are more than twice the size of *C. cayetanensis (*Dubey et al., 2019). *Cryptosporidium* spp., another coccidian, can also parasitize the human intestinal tract and biliary system, but *Cryptosporidium* stages characteristically occupy the microvillous border.

The identity of the parasite in the present case was confirmed by molecular detection using real-time PCR. The specificity of the real-time assay was previously evaluated by Murphy et al. (2017) analyzing purified DNA from 11 protozoan parasites (*Giardia intestinalis, Blastocystis hominis, Cryptosporidium parvum, Cryptosporidium hominis, Entamoeba histolytica, Plasmodium falciparum, Eimeria acervulina, Eimeria tenella, Eimeria maxima, Toxoplasma gondii,* and *Trypanosoma cruzi*). No cross-reactivity was observed with other known simian *Cyclospora* species (*C. cercopitheci, C. colobi,* and *C. papionis*) (Murphy et al., 2017).

The observations reported here could help pathologists to recognize *C. cayetanensis* stages using light and electron microscopy.

ACKNOWLEDGMENTS

We thank Camila Cezar, Fernando Murata, and Oliver Kwok for assistance. This study used archived material. No human experiments were performed.

LITERATURE CITED

Almeria, S., H. N. Cinar, and J. P. Dubey. 2019. *Cyclospora cayetanensis* and cyclosporiasis: An update. Microorganisms 7: 317. doi:10.3390/microorganisms7090317

Bendall, R. P., S. Lucas, A. Moody, G. Tovey, and P. L. Chiodini. 1993. Diarrhoea associated with cyanobacterium-like bodies: A new coccidian enteritis of man. Lancet 341: 590–592.

Connor, B. A., J. Reidy, and R. Soave. 1999. Cyclosporiasis: Clinical and histopathologic correlates. Clinical Infectious Diseases 28: 1216–1222.

De Górgolas, M., J. Fortés, and M. L. Fernández Guerrero. 2001. *Cyclospora cayetanensis* cholecystitis in a patient with AIDS. Annals of Internal Medicine 134: 166. doi:10.7326/0003-4819-134-2-200101160-0021

Di Gliullo, A. B., M. S. Cribari, A. J. Bava, J. S. Cicconetti, and R. Collazos. 2000. *Cyclospora cayetanensis* in sputum and stool samples. Revista do Instituto de Medicina Tropical de São Paulo 42: 115–117.

Dubey, J. P., and S. Almeria. 2019. *Cystoisospora belli* infections in humans: The past 100 years. Parasitology 146:1490–1527.

Dubey, J. P., K. J. Evason, and Z. Walther. 2019. Endogenous development of *Cystoisospora belli* in intestinal and biliary epithelium of humans. Parasitology 146: 865–872.

Dubey, J. P., D. S. Lindsay, M. C. Jenkins, and C. Baur. 2020. Biology of intestinal coccidia. *In* Coccidiosis in livestock, poultry, companion animals, and humans, J. P. Dubey (ed.). CRC Press, Taylor & Francis Group, Boca Raton, FL, p. 1–36.

Giangaspero, A., and R. B. Gasser. 2019. Human cyclosporiasis. Lancet Infectious Diseases 19: e226–e236. doi:10.1016/S1473-3099(18)30789-8

Hussein, E. M., A. H. Abdul-Manaem, and S. L. El-Attary. 2005. *Cyclospora cayetanensis* oocysts in sputum of a patient with active pulmonary tuberculosis, case report in Ismailia, Egypt. Journal of the Egyptian Society of Parasitology 35: 787–793.

Li, J., R. Wang, Y. Chen, L. Xiao, and L. Zhang. 2020. *Cyclospora cayetanensis* infection in humans: Biological characteristics, clinical features, epidemiology, detection method and treatment. Parasitology. 147: 160–170.

Murphy, H., R. S. Lee, and A. J. da Silva. 2017. Evaluation of an improved U.S. Food and Drug Administration method for the detection of *Cyclospora cayetanensis* in produce using real-time PCR. Journal of Food Protection 80: 1133–1144.

Nhieu, J. T. V., F. Nin, J. Fleury-Feith, M. T. Chaumette, A. Schaeffer, and S. Bretagne. 1996. Identification of intracellular stages of *Cyclospora* species by light microscopy of thick sections using hematoxylin. Human Pathology 27: 1107–1109.

Ortega, Y. R., R. Nagle, R. H. Gilman, J. Watanabe, J. Miyagui, H. Quispe, P. Kanagusuku, C. Roxas, and C. R. Sterling. 1997. Pathologic and clinical findings in patients with cyclosporiasis and a description of intracellular parasite life-cycle stages. Journal of Infectious Diseases 176: 1584–1589.

Ortega, Y. R., C. R. Sterling, R. H. Gilman, V. A. Cama, and F. Díaz. 1993. *Cyclospora* species—A new protozoan pathogen of humans. New England Journal of Medicine 328: 1308–1312.

Sifuentes-Osornio, J., G. Porras-Cortés, R. P. Bendall, F. Morales-Villarreal, G. Reyes-Terán, and G. M. Ruiz-Palacios. 1995. *Cyclospora cayetanensis* infection in patients with and without AIDS: Biliary disease as another clinical manifestation. Clinical Infectious Diseases 21: 1092–1097.

Sun, T., C. F. Ilardi, D. Asnis, A. R. Bresciani, S. Goldenberg, B. Roberts, and S. Teichberg. 1996. Light and electron microscopic identification of *Cyclospora* species in the small intestine. Evidence of the presence of asexual life cycle in human host. American Journal of Clinical Pathology 105: 216–220.

Tsang, O. T. Y., R. W. C. Wong, B. H. S. Lam, J. M. C. Chan, K. Y. Tsang, and W. S. Leung. 2013. *Cyclospora* infection in a young woman with human immunodeficiency virus in Hong Kong: A case report. BMC Research Notes 6: 521. doi:10.1186/1756-0500-6-521

Velásquez, J. N., S. Carnevale, M. Cabrera, L. Kuo, A. Chertcoff, M. Mariano, J. P. Bozzini, C. Etchart, R. Argento, and C. di Risio. 2004. *Cyclospora cayetanensis* en pacientes con SIDA y diarrea crónica. Acta gastroenterologica Latinoamericana 34: 133–137.

Verweij, J. J., D. Laeijendecker, E. A. Brienen, L. Van Lieshout, and A. M. Polderman. 2003. Detection of *Cyclospora cayetanensis* in travellers returning from the tropics and subtropics using microscopy and real-time PCR. International Journal of Medical Microbiology 293: 199–202.